Received: 28 October 2017 | Revised: 2 April 2018 | Accepted: 18 May 2018

DOI: 10.1002/cnm.3107

RESEARCH ARTICLE - FUNDAMENTAL

WILEY

Finite element analysis of the influence of three-joint spinal complex on the change of the intervertebral disc bulge and height

Klaudia Szkoda-Poliszuk | Małgorzata Żak | Celina Pezowicz

Department of Biomedical Engineering, Mechatronics and Theory of Mechanisms, Faculty of Mechanical Engineering, Wroclaw University of Science and Technology, Wrocław, Poland

Correspondence
Klaudia Szkoda-Poliszuk, Department of Biomedical Engineering, Mechatronics and Theory of Mechanisms, Faculty of Mechanical Engineering, Wroclaw University of Science and Technology, Wrocław, Poland.
Email: klaudia.szkoda@pwr.edu.pl

Funding information
Wroclaw Centre for Networking and Supercomputing, Grant/Award Number: 423

Abstract

This study evaluated the changes of height and bulging occurring in individual layers of the annulus fibrosus of the intervertebral disc for 3 load scenarios (axial compression, flexion, and extension). The numerical model of a single motion segment of the thoracic spine was analysed for 2 different configurations, ie, for the model of a physiological segment and a segment with the posterior column removed. In the physiological segment, all annulus fibrosus layers decrease in height regardless of the applied load, bulging outside the intervertebral disc. Removal of the posterior column increases mobility and disrupts the load transfer system, with the lamellae bulging into the intervertebral disc.

KEYWORDS

bulging disc, finite element method, intervertebral disc, thoracic spine segment, 3-joint complex

1 | INTRODUCTION

As a part of the human locomotor system, the spine has a very complex structure. It fulfils some basic functions in the human body. First of all, it protects the spinal cord, providing appropriate mobility of the spinal column. In addition, a key function of the spine is the transfer of loads along its axis.[1,2] The complex structure of the spine consists of alternating vertebrae, which are rigid bone elements, and intervertebral discs (IVD), which act as susceptible elastic elements. Transfer of loads along the spine axis is possible thanks to the 3-joint complex (the "articular triad"), which is the basic anatomical and functional unit of the spine. The 3-joint complex consists of the IVD and 2 symmetrical facet joints, which connect adjacent vertebrae. The method of support of spinal motion segments has a significant effect on the kinematics of the spine and the mechanical properties of the IVD.[3,4] With respect to location of the points of support, the spine is divided into the anterior and posterior columns.[5]

The anterior column of the spine consists of vertebral bodies with intervertebral discs. It is primarily responsible for the transfer of loads along the long axis of the human body during both static and dynamic activities. Multiplane kinematic movements are possible thanks to the IVD because of its complex structure consisting of the annulus fibrosus (AF) and the nucleus pulposus (NP). The AF not only shields the NP and maintains its shape but also stabilises and reduces mobility of the adjacent vertebrae. The basic element of the AF is an organised structure of collagen fibres embedded in a highly hydrated matrix consisting of water, proteoglycans, and noncollagen fibres. Under the influence of axial loads of a functional spinal unit (FSU), the lamellae of the AF bulge out in the horizontal plane (on the outside of the disc).

A very important role in the transfer of loads and reduction of excessive mobility of the spine is played by the posterior column, which consists of vertebral arches and articular processes of individual functional spinal units. According to a study by Nachemson,[6] articular processes transfer about 20% of the acting compression load while White and Panjabi[1] showed that the load on articular processes, especially in the lumbar spine, may reach up to do 33% of the body weight. In addition, Adams et al[7] found that in the case of a healthy spine, the posterior column accounts for 5% to 10% of the acting load in the load transfer system. The amount of the posterior column load increases to over 40% in the case of the occurrence of degeneration of the IVD.[8]

The results of experimental studies and numerical simulations of the load transfer system of the spinal joints show that the load acting on the spine is transferred mainly by the IVD. On the other hand, the share of the articular processes increases with the appearance of the shear force, whose value depends on the body posture. Shirazi-Adl[9] showed that extension bending moment increases the load acting on the articular processes in the range of 10% to 30%. In the case of flexion, the maximum load transferred by the articular processes appears at a bend in the range of 10° to 12° and in the presence of additional shear force. This demonstrates that the articular processes transfer a substantial part of the load, both during flexion and extension.

Most studies confirm the essential, even crucial role of the IVD in the correct functioning of the spine. The studies analysing the impact of anterior and posterior columns in the load transfer system estimate the percentage share of those elements on the basis of global changes in displacement of the IVD or the change of intradiscal pressure. On the other hand, there is lack of analysis showing the changes that occur inside the disc depending on the support system.

Therefore, this study evaluated the changes occurring in individual layers of the AF of the IVD for 3 load scenarios (axial compression, flexion, extension). The changes of height and bulging in AF lamella were analysed on the model of a single thoracic FSU for 2 different configurations, ie, for the model of a physiological segment and a segment with the posterior column removed. The thoracic FSU (Th11-Th12) was analysed because of its unique location in the column of the spine (the last segment in the thoracic spine). As is known, the spine has several characteristic places which are a natural transition between the subsequent segments (among others from the thoracic to the lumbar), and each segment is characterised by a difference of geometric parameters, resulting from the load transmission. These changes cause disturbances in the continuity of load transmission, thereby increasing the instability of the connection.

2 | MATERIAL AND METHODS

2.1 | Development of FE models

The spatial (3D) numerical model of the thoracic FSU (Th11-Th12) was built on the basis of spinal dimensions obtained from analysis of CT images. The CT study was performed on 2 men aged 40 to 50 years who had no changes in the osteoarticular system of the spine. In both cases, the diagnostics was carried out at the same lateral resolution (0.37 mm) and thickness of the layer (0.74 mm). The cross-sectional images (2D) were imported into the InVesalius software, which was used to create 3D models of the Th11 and Th12 vertebrae.[10] The dimensions of both vertebrae (Figure 1) were derived from measurements of 3D models. The values of individual parametric dimensions of the vertebrae included in the numerical model (Table 1) were verified with the vertebral dimensions found in the literature.[11-13]

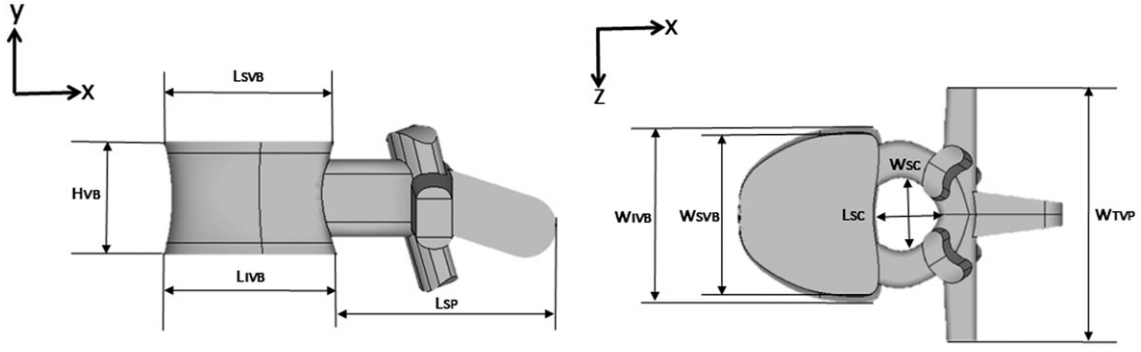

FIGURE 1 Selected thoracic vertebrae parametric dimensions: L_{SVB}, superior vertebral body length; W_{SVB}, superior vertebral body width; L_{IVB}, inferior vertebral body length; W_{IVB}, inferior vertebral body width; H_{VB}, vertebral body height; L_{SC}, spinal canal length; W_{SC}, spinal canal width; W_{TVP}, transverse process width; L_{SP}, spinous process length

TABLE 1 The values of parametric dimensions of the vertebrae included in the numerical model

	L_{SVB} (mm)	W_{SVB} (mm)	L_{IVB} (mm)	W_{IVB} (mm)	H_{VB} (mm)	L_{SC} (mm)	W_{SC} (mm)	W_{TVP} (mm)	L_{SP} (mm)
Th11	31.9	34.9	31.8	39.1	21.3	15.9	17.0	30.0	48.8
Th12	32.8	39.0	33.4	42.1	22.7	16.4	18.0	31.0	49.4

The geometry of the model of the Th11-Th12 thoracic FSU was created and calculated in the ANSYS Mechanical APDL 16.2 software. The vertebrae and the IVD were described by 10-node, tetrahedral solid elements (SOLID187) with 3 degrees of freedom at each node. Each vertebral body was modelled as cancellous bone surrounded by a layer of cortical bone with the thickness in the range of 0.5 to 0.6 mm.[14] The study took into account the presence of endplates (superior and inferior) in both vertebrae as well as interspinous cartilage connecting articular processes. The thickness of the endplate was modelled as 10% of the vertebral body height, according to the published mean values.[15] All 4 main types of ligaments present in the spine (anterior longitudinal ligaments (ALL), posterior longitudinal ligaments (PLL), intertransverse ligaments (ITL), interspinous ligaments (ISL)) were modelled as 2-node link element type LINK10. This element permits only uniaxial tension or compression with 2 degrees of freedom at each node. The individual components of a model of a thoracic FSU are shown in Figure 2.

2.2 | Material properties

The bone tissue of the vertebrae and endplates and the interspinous cartilage was described by isotropic, linear-elastic material properties.[16-27] The IVD was modelled in accordance with the vertebral model proposed by Schmidt et al,[28] who modelled the structure of the AF as a matrix strengthened with layers of collagen fibres. The matrix of the AF surrounding the NP was described by isotropic, linear-elastic material properties.[16,17,20,22,23,29-31] Six cylindrically arranged layers of collagen fibres were modelled in the AF matrix, which were radially placed between successive annuli fibrosis (lamellae). Layers of fibres were assigned isotropic, linear material properties with the initial angular orientation of each fibre and theoretical defined cross-sectional area.[23,29,30,32-34] The fibres were tilted at a 30° degree and arranged alternately, ie, to the right or to the left.[3] Ligaments (ALL, PLL, ISL, ITL) were also described by isotropic, linear material properties with theoretical defined cross-sectional area.[17,19,20,31,32] The articulating facet surfaces were modelled using surface-to-surface contact elements (with a penalty algorithm and a friction coefficient of 0.1). The material properties of the individual tissue structures are shown in Table 2.

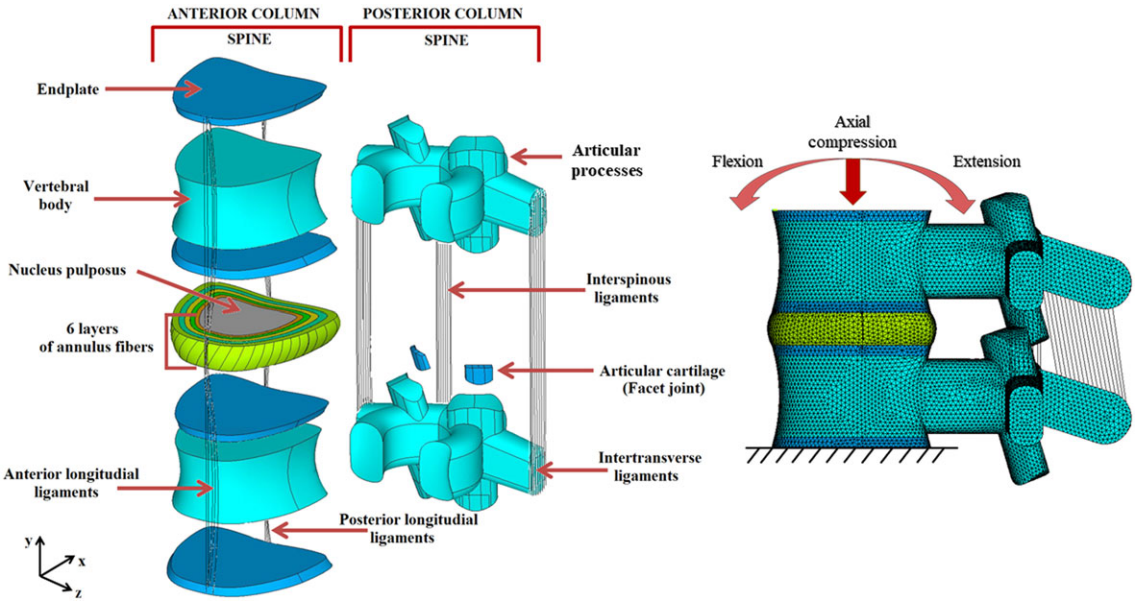

FIGURE 2 The individual components of a thoracic FSU

TABLE 2 The material properties of the components of a FSU

	Young's Modulus (MPa)	Poisson's Ratio (-)	Cross Section (mm^2)	References
SOLID component name				
Cortical bone	12 000	0.3		16-20
Cancellous bone	100	0.2		16,18,21
Articular processes	3500	0.25		18,20,22,23
Endplate	25	0.1		22-24
Nucleus pulposus	1	0.499		17,20,22,23,29-31
Annulus ground substance	4.2	0.45		16,17,20,22,23,29-31
Interspinous cartilage	33	0.3		20,25-27
LINK component name				
Annulus fibre				
Layer 1	550	0.45	0.02	23,29,30,32-34
Layer 2	495			
Layer 3	440			
Layer 4	420			
Layer 5	385			
Layer 6	360			
Anterior longitudial ligaments	20	0.3	64	17,19,20,31,32
Posterior longitudial ligaments	50	0.3	20	
Interspinous ligaments	12	0.3	40	
Intertransverse ligaments				

2.3 | Boundary and loading conditions

The numerical simulations were performed for 2 configurations: the physiological FSU, in which the load is transferred by the anterior and posterior columns (Figure 2), and the FSU with the posterior column removed. In the first stage, the analysis of both configurations was carried out for the compression load acting with the axial force of 650 N.[27,35,36] This force corresponds to the load transferred by the lumbar spine of an average adult, resulting from the weight of the trunk, head, and upper limbs. In subsequent stages, the analysis was carried out for the load simulating flexion as well as extension, acting with the moment of force equal to 10 Nm, as it has been recommended by Panjabi et al.[37] Both in the case of compression as well as flexion and extension, the load was applied to the surface of the superior endplate of the vertebral body Th11.[38] In each of the cases, the models were mounted by removing all degrees of freedom of the nodes on the surface of the inferior endplate of the vertebral body Th12.

3 | RESULTS

The performed numerical simulations were used to determine the change in the distribution of displacements in the IVD, thus establishing the height (H_l) of individual layers of the AF with respect to the horizontal plane (Figure 3A) and the bulging (B_l) of the layers with respect to the sagittal plane (Figure 3B). Depending on the bulging direction of individual layers of the AF, their values were presented as positive (the layer bulged outside the disc) or negative (layer bulged into the disc) (Figure 3C). The height (H_l) of successive layers of the AF was determined as the difference between the height of IVD before loading equal to 7 mm and change in height. Similarly, the bulging (B_l) of successive layers of the AF was determined as the difference between layer position before loading relative to the *x*-axis and layer position after loading relative to the *x*-axis. All analysed parameters were determined for both analysed configurations of a FSU (physiological and with the posterior column removed) in 3 loading stages: axial compression (a), flexion (b), and extension (c).

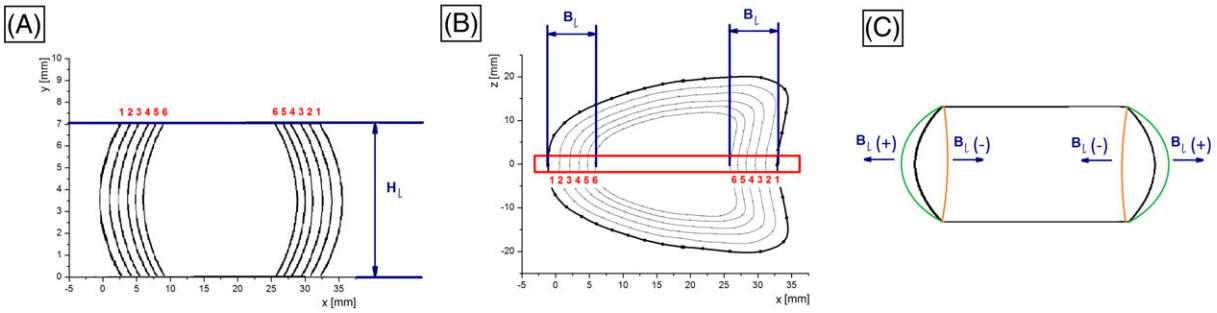

FIGURE 3 The area of analysis of the mechanical parameters of the IVD: A, height H_l in the horizontal plane, B, bulging B_l in the sagittal plane, and C, bulging direction B_l, where (+) means bulging outside the disc and (−) means bulging into the disc

3.1 | Change in the height of individual layers of the AF of the IVD

The analysis showed that in the segment with the preserved articular triad, all layers of the AF decrease in height regardless of the applied load (Figure 4). Moreover, the existing differences in height change depend on the type of load and the analysed area (anterior or posterior part of the disc). In the anterior part of the disc, the greatest changes in the height of individual layers were observed for flexion, where they are almost twice as large as those for extension. In the posterior part of the disc, the obtained values are similar for all load conditions. Because of axial compression (Figure 4A), the layers in the anterior part are characterised by a greater decrease in height than the layers in the posterior part. The height change in the first layer (in the anterior part $\Delta H_1 = 0.39$ mm, in the posterior part $\Delta H_1 = 0.12$ mm) is more than twice smaller compared to the other 5 layers. In the case of flexion of the physiological segment, there were also smaller observed changes of disc height within the first layer (in the anterior part $\Delta H_1 = 0.54$ mm, in the posterior part $\Delta H_1 = 0.10$ mm). By contrast, the greatest value in the anterior part was obtained for the second and third layers, where the height change $\Delta H_{2,3}$ is 0.96 mm (Figure 4B). Analysis of the results obtained during extension showed that the load acting mainly on the posterior part of the disc does not result in increased height change in that part relative to the results obtained for compression and flexion (Figure 4C). These results are similar for all 3 load conditions. In addition, it was noted that in the anterior part of the disc, the changes in height are lower in value than in the case of compression or flexion. It was demonstrated that the height change in the first layer (in the anterior part $\Delta H_1 = 0.29$ mm, in the posterior part $\Delta H_1 = 0.13$ mm) is also the smallest compared to the other 5 layers.

Removal of the posterior column from a FSU caused a significant change in the system of load transfer through the structures of the IVD (Figure 4). Axial compression (Figure 4A) affects the uniform course of the height change in the anterior and posterior parts of the AF of the IVD. The height change is practically constant throughout the disc volume. It was demonstrated that the values of height change in the first layer (in the anterior part $\Delta H_1 = 0.27$ mm, in the posterior part $\Delta H_1 = 0.24$ mm) are twice smaller compared to the other 5 layers. Analysis of the results obtained in the case of flexion (Figure 4B) and extension (Figure 4C) of the segment with the posterior column removed showed that, depending on the direction of the moment of force, the AF is compressed on one side and tensed on the other side, which translates into significant changes in its height. Flexion leads to greatest height changes in the anterior part of the IVD. Those values are almost 4 times greater than the values obtained in the case of axial compression. The greatest value of height change was observed for the second layer, where ΔH_2 equals 2.07 mm in the anterior part and 0.48 mm in the posterior part. In the case of extension, the biggest changes in height occurred in the posterior part of the disc, in particular in the second layer, where in the anterior part $\Delta H_2 = 1.27$ mm and in the anterior part $\Delta H_2 = 0.50$ mm.

3.2 | Change in the bulging of individual layers of the AF of the IVD

In addition, it should be noted that during axial compression of both analysed configurations of the FSU, the bulging of subsequent layers of the AF decreases towards the structures of the NP (Figure 5A). In both configurations, the bulging values obtained for individual layers are similar to each other both in the anterior and posterior parts. In the physiological segment, the greatest bulging occurs within the second layer, where in the anterior part $B_2 = 0.69$ mm and in the posterior part $B_2 = 0.55$ mm. By contrast, in the motion segment with the posterior column

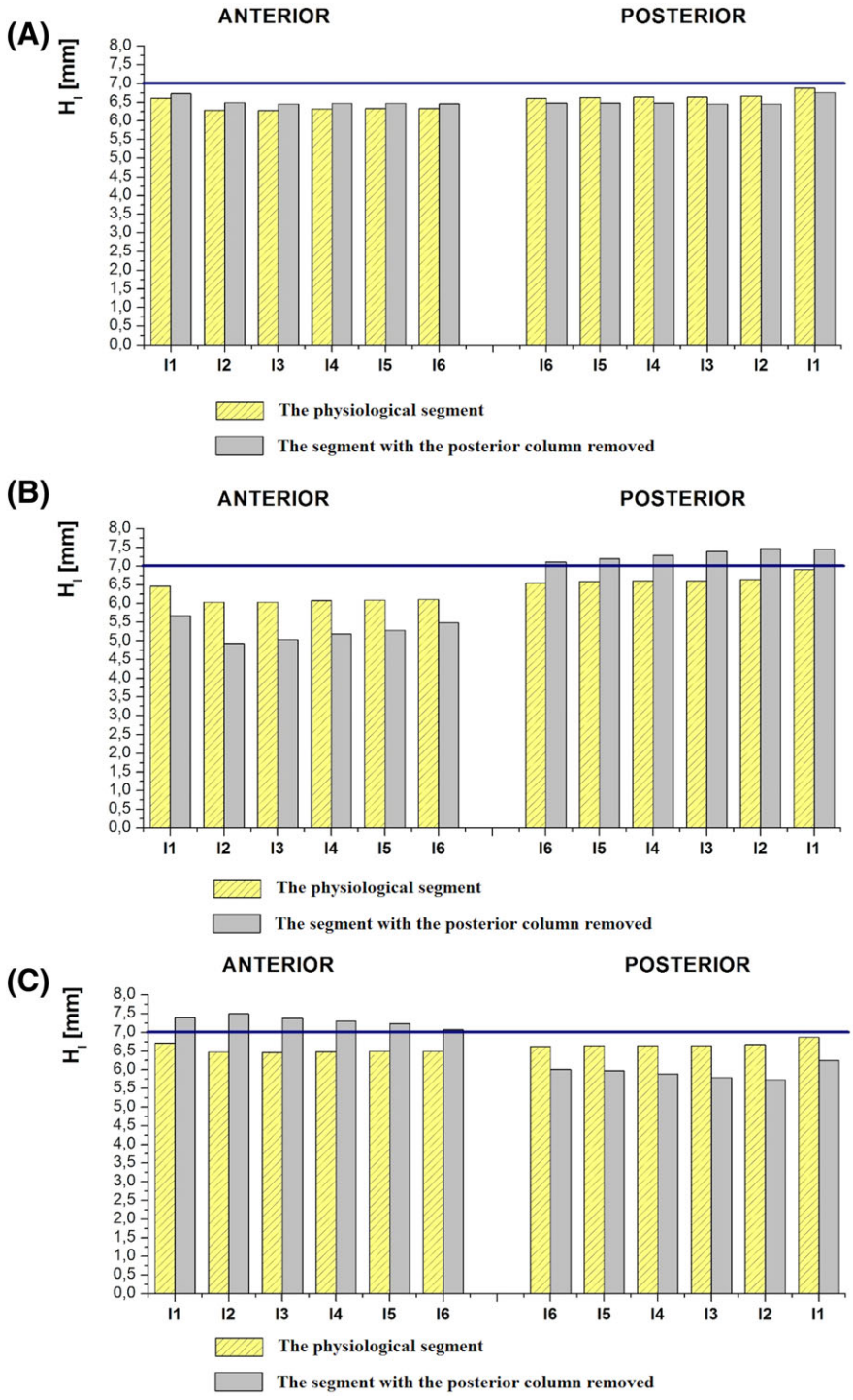

FIGURE 4 The change in height of the individual layers of the AF of both analysed configurations during A, axial compression, B, flexion, and C, extension, where H_l is the height of the AF layer after loading and $l\varepsilon\{1, 2, 3, 4, 5, 6\}$ are individual layers of the AF

removed, the greatest bulging in the anterior part was observed also in the second layer ($B_2 = 0.62$ mm), while in the posterior part, it was observed in the first layer ($B_1 = 0.69$ mm). At the same time, there is a visible impact of the posterior spinal column, which results in an increased bulging in the anterior part of the IVD, especially within the 3 external layers.

It was noted that during flexion, the load is transferred to a greater extent by the anterior part of the IVD (Figure 5B). This is evidenced by the bulging values obtained for the individual layers, ranging from 1.08 to 0.83 mm for the physiological segment and from 1.84 to 1.00 mm for the with the posterior column removed. At the same time, the bulging of the layers in the anterior part is greater in the segment with the posterior column removed. Moreover, it should be noted that in the posterior part of the disc, 3 outer layers bulge into the disc in contrast to the physiological segment, in which all layers bulge out of the disc.

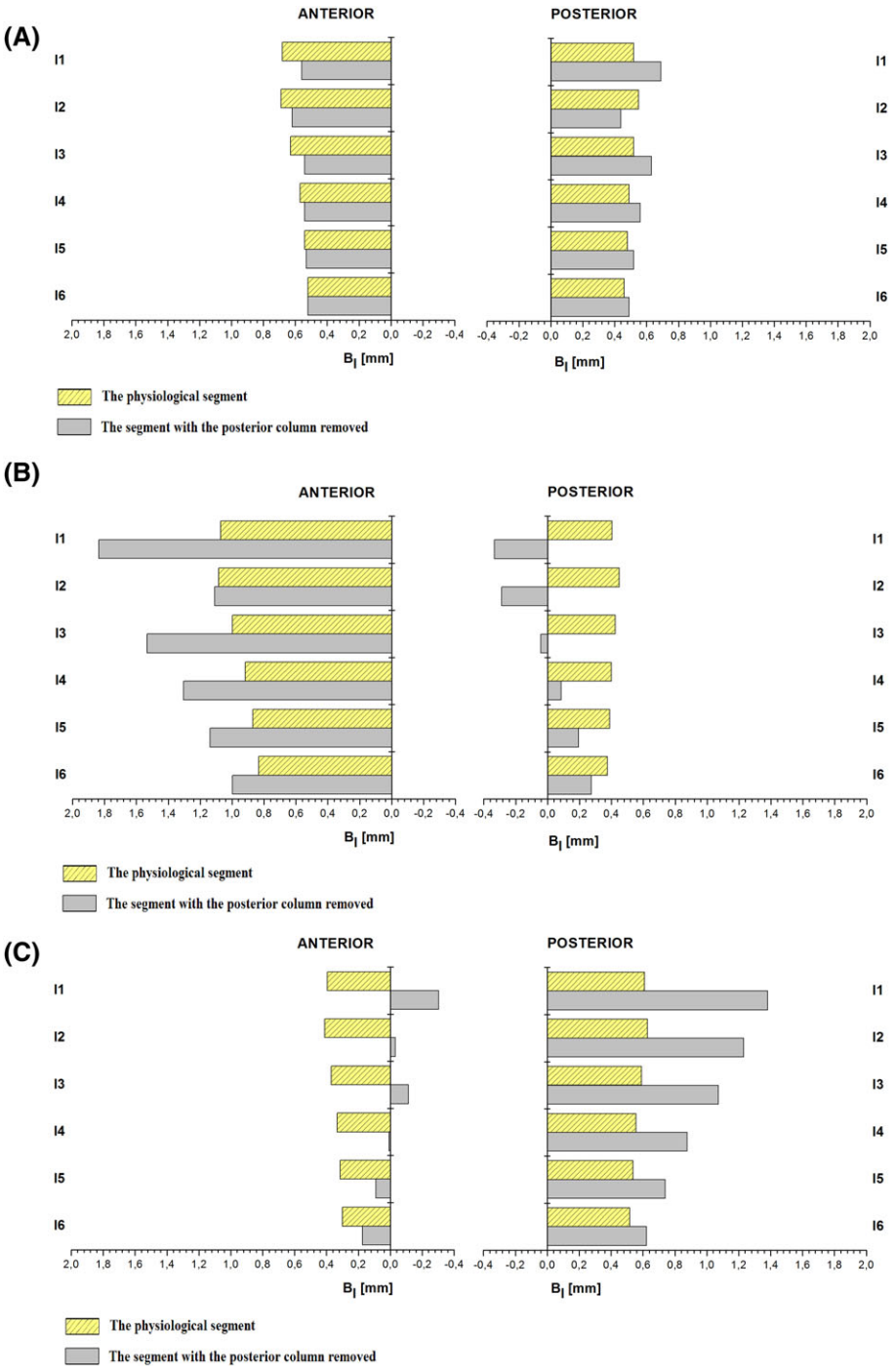

FIGURE 5 The bulging of the individual layers of the AF of both analysed configurations during A, axial compression, B, flexion, and C, extension, where B_l is the bulging of the AF layer and $l \in \{1, 2, 3, 4, 5, 6\}$ are individual layers of the AF

As in the case of flexion, during extension (Figure 5C), the removal of the posterior column in the motion segment increased the value of bulging in the posterior part relative to the physiological segment. The changes in the bulging of the layers of the AF in both analysed configurations of the motion segment indicated that loading during extension is transferred to a greater degree by the posterior part of the IVD (Figure 5C). This is evidenced by the bulging values obtained for the individual layers, ranging from 0.63 to 0.52 mm for the physiological segment and from 1.38 to 0.62 mm for the posterior column removed. In the anterior part of the disc, the 3 outer layers are characterised by bulging into the disc in contrast to the physiological segment, in which all layers bulge out of the disc.

4 | DISCUSSION

The conducted tests allowed us to observe changes caused by transfer of loads by the spinal motion segment not only in the outer but also in the inner layers of the IVD. The processes taking place within the IVD are extremely important because most of the degenerative changes start with the changes occurring on the border of the nucleus and the AF.[39,40] In addition, it is worth noting that the damage in the form of delamination of the AF lamellae occurs mainly in the posterior part of the IVD, resulting in loss of coherence between the adjacent lamellae.[39-42] In the available literature, the experimental studies conducted on spinal motion segments mostly concern only analyses of global changes of the mechanical parameters of the IVD, without taking into account changes in both external and internal layers. Therefore, this study used the finite element method, which enabled analysis of the changes occurring in each layer of the IVD, which is an important cognitive element in the biomechanics of the IVD.

The research presented in this study demonstrated that, under the influence of the load acting on the physiological motion segment with the preserved complete articular triad, each of the individual layers of the AF decreases in height, bulging out of the disc (Figures 4 and 5). In addition, the acting load compresses the NP and pushes it towards the AF lamellae, which bulge out under the pressure. This process also leads to an increase in intradiscal pressure.[6,8,43,44] Depending on the acting load, the NP moves towards the anterior part (during flexion) or posterior part (during extension) of the disc. In the case of complex load conditions, the nucleus also exerts pressure on lateral parts of the IVD. Moreover, under the influence of compression load, collagen fibres of the AF reduce the angle of inclination with respect to the vertebral body surfaces by about 3°,[45] which also affects the bulging of the AF lamellae outside the disc. It should be noted here that the values of the parameters H_l and B_l were interpreted only from finite element mesh nodes in the sagittal and horizontal plane of the IVD. The changes in the frontal plane are not presented. The obtained results are the values read from a certain range (Figure 3B) in a 2-dimensional system (sagittal and horizontal plane). Therefore, the parameters describing the changes in the geometry of the IVD, caused by the acting load, were determined in the radial direction (bulging) and in the axial direction (height). The analysis of the obtained results did not take into account 3-dimensional changes in the disc geometry, also occurring in the circumferential direction. The conducted studies also demonstrated that the value of the bulging of successive layers in the IVD decreases towards the structures of the NP regardless of the status of the load acting on the physiological motion segment, which was also demonstrated in a study by Heuer et al.[46] However, Heuer et al[46] analysed only global changes occurring in the outer and inner structures of the disc, without considering the division into its individual layers and without distinguishing between the anterior and posterior parts of the IVD. The presented research shows that during axial compression (with a force of 650 N), the average bulging value in the case of the physiological motion segment in the anterior part of the disc amounts to 0.61 ± 0.06 mm and is greater than in the posterior part (0.50 ± 0.03 mm). The obtained values are very close to the bulging values obtained by Denoziere et al,[47] who showed in numerical tests that bulging of the disc (during axial compression with the force of 720 N) falls in the range of 0.4 mm (side part of the disc) to 0.7 mm (posterior part of the disc). Fredericson et al[48] in their experimental tests observed that in the early morning hours, the bulging of the posterior part of the IVD takes lower values than after 6 hours of daily activity. They also noted that immediately after awakening and getting up, the average bulging value across the entire IVD amounts to 1.8 mm during flexion and 0.9 mm during extension. It should also be noted that, according to the conclusions of Fredericson et al,[48] it is unclear to what extent flexion or extension influence bulging of the posterior part of the IVD. This research shows that during flexion, the average bulging value in the case of the physiological motion segment in the anterior part of the disc is greater than in the posterior part. The bulging values are smaller for the extension in the anterior part decreases with the approach to the NP structures of the disc than for the posterior part. The results obtained by Fredericson et al[48] are significantly higher than the values observed in the presented tests. This may be because of the fact that Fredericson et al[48] used magnetic resonance imaging (MRI) to analyse the changes in the geometry of the IVD. Determination of the values of geometric parameters by analysing MRI images can result in measurement inaccuracies because of insufficient resolution of the obtained images or low accuracy of the marked contours of the analysed tissues.

In a segment without a complete articular triad, the load transfer function is taken over in its entirety by the IVD. This involves an increased motion within the segment as the primary role of the articular processes is to stabilise the spine and eliminate its axial rotation during flexion and extension.[49] Therefore, the removal of the posterior column results in greater changes to the analysed parameters with respect to the physiological segment. Those changes are especially noticeable during flexion and extension and are characterised by a greater decrease of the height and a greater bulging of the IVD in the anterior or posterior parts (Figures 4 and 5). In addition, the tests show that in both cases, the differences in the values of the analysed parameters between the anterior and posterior parts were greater in the

segment with the posterior column removed than in the physiological segment. In the motion segment with the posterior column removed, the average bulging values were, respectively, 0.56 ± 0.03 mm for the anterior part and 0.55 ± 0.08 mm for the posterior part. Heuer et al[50] conducted tests on lumbar motion segments with the posterior columns removed and found out that axial compression with the force of 500 N for 15 minutes decreased the height of the IVD by 1.14 mm. The researchers also noticed that the anterior part of the disc was bulging out more (0.86 mm) than the posterior part (0.45 mm). The bulging value obtained by Heuer et al[50] for the posterior part of the disc is similar to the value obtained in this study. However, the bulging value obtained in the anterior part of the disc is significantly greater (by about 0.40 mm).

It should be stressed that the IVD changes its height under the influence of the load acting on its structures; this height is associated with the bulging of the AF lamellae outward or inward the disc. The change in height (H_l) of the outer (l_1), medium (l_3), and inner layers (l_5) of the IVD is associated with its bulging (B_l) during flexion and extension (both analysed configurations of the model) shown in Figures 6A and 7A. Therefore, it can be concluded that the bulging increases with a reduction in the disc height. It should also be noted that the removal of the posterior column from the FSU disturbs the system of load transfer through the spinal structures as, depending on the acting load, the outer layers of the disc bulge inward in its anterior (Figure 7A) or posterior part (Figure 6A). As mentioned above, bulging of AF layers inward the disc is dangerous because it can lead to delamination of the AF lamellae and consequently to degenerative changes of the disc. Excessive bulging of the anterior or posterior part of the disc in the segment with the posterior column removed is reflected in the distribution of strain presented in the cross section relative to the sagittal plane in Figures 6B and 7B. As a consequence of the removal of the posterior column, there is an almost twice bigger strain (maximum value of 0.39) observed in the anterior part of the IVD during flexion compared with the physiological segment (maximum value of 0.17) (Figure 6B). A similar trend can be observed during extension. Strain of the posterior part of the IVD (maximum value of 0.22) is also more than double that of the physiological segment (maximum value of 0.09) (Figure 7B). The conducted research also showed that the disc bulging in the motion segment with the posterior column removed was about 3% greater during flexion and about 10% greater during extension in relation to the disc bulging in the physiological mobility segment.

Understanding the role of the IVD in the load transfer system through the spine is particularly important because of the increasing percentage of degenerative diseases in society. The first stage of degenerative changes of the IVD is its dehydration, which results in a reduction of the disc height and its significant bulging outward of the IVD.[51,52] This leads to further changes, including on the change of the geometry of the FSU, which according to the studies negatively affects adjacent segments.[53,54] MRI diagnostics provides us only with information about the direction of changes, resulting from dehydration. However, it does not give an explanation of the course of this process in the entire IVD volume. Analysis of the segment without a complete articular triad (with the posterior column removed) reflects to some

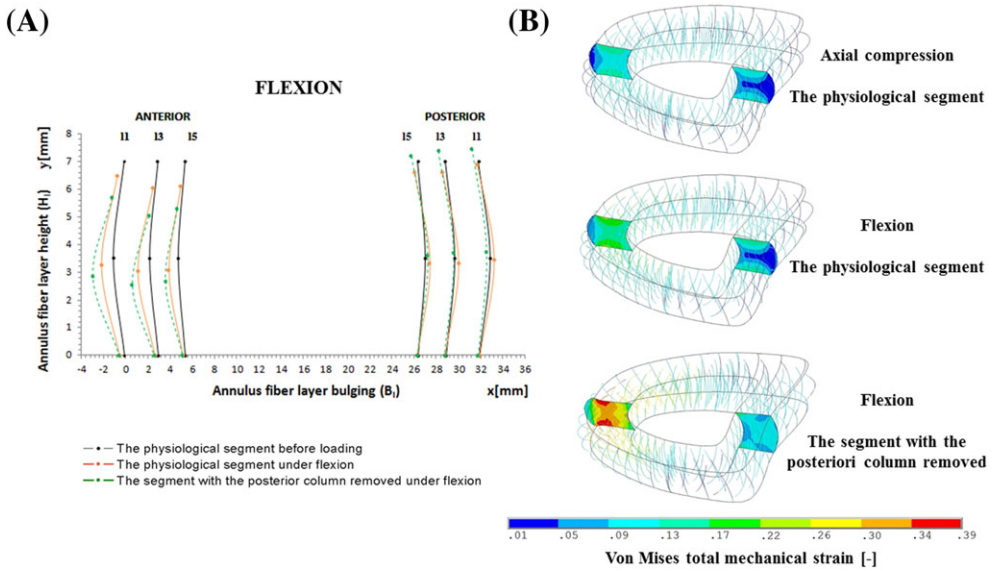

FIGURE 6 The height changes (H_l) and bulging (B_l) of AF layers of the IVD in the sagittal plane (A) and distribution of strain according to the Huber-von Mises hypothesis in fibre layers of the IVD in the cross section relative to the sagittal plane (B) during flexion of the motion segment

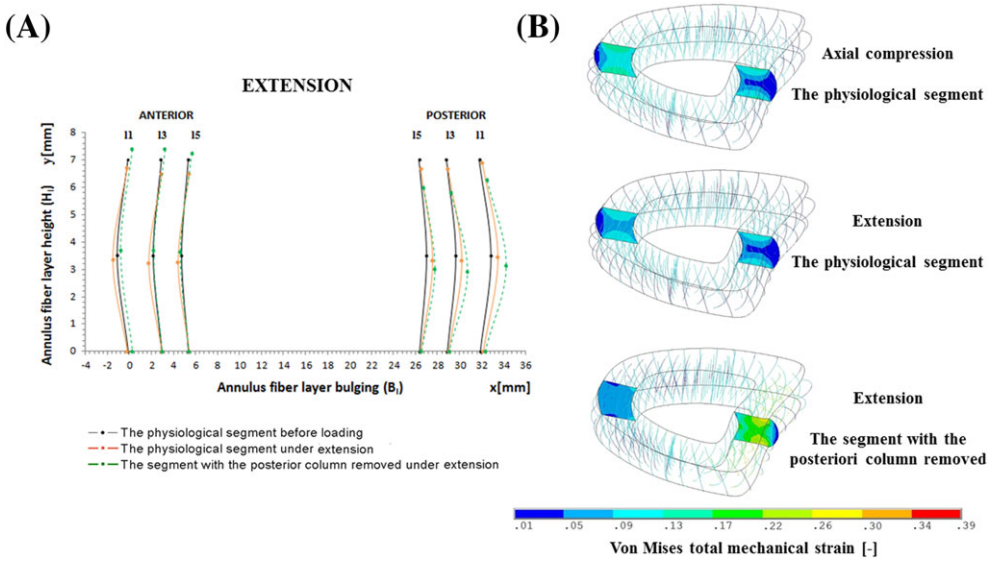

FIGURE 7 The height changes (H_l) and bulging (B_l) of AF layers of the IVD in the sagittal plane (A) and distribution of strain according to the Huber-von Mises hypothesis in fibre layers of the IVD in the cross section relative to the sagittal plane (B) during extension of the motion segment

extent the case of surgical treatment associated with the facetectomy procedure.[55,56] Facetectomy is performed to decompress the nervous system and reduce pressure on the spinal cord. Analyses using the finite element method allow to determine the qualitative and quantitative changes of the individual AF lamellae, which are caused by a disturbance in the load transfer system.

It should be noted that the conducted tests allowed us to learn about the phenomena occurring within the IVD structures and also complemented the existing analyses presented in the literature. Although the presented solution to the problem was in some aspects simplified, which is a limitation of the analysis, the proposed model allowed the demonstration of the impact of the load transfer by the posterior column of the spine on the changes occurring in the individual layers of the AF of IVD. In particular, the properties of the bone tissue, the nucleus pulposus, and the matrix of the AF were adopted as the properties of the isotropic material. However, the changes occurring within the vertebral bone tissue were not the subject of the ongoing research. Consequently to optimise the time of the conducted numerical simulations, the vertebral bone tissue was described as linear properties. The IVD was the structure subjected to detailed analysis; therefore, the study focused on its accurate reproduction by modelling in it collagen fibres as linear elements with variable material properties. The outer lamellae of the AF have higher mechanical properties than the lamellae located closer to the NP (Table 2). This allowed to model the physiological structure of IVD. Because of the fact that collagen fibres embedded in AF lamellae play the greatest role in the IVD, the structures of the NP and of the AF matrix have also been simplified. Modelling of these structures as linear elements is also proposed by authors of other studies.[20,22,23,29-32]

5 | CONCLUSION

Analysis of the presented results for both analysed configurations of the motion segment shows that articular processes play a huge role in the transfer of loads by the spine. They provide an additional support for the spinal column, especially during the action of the load forcing flexion as well as extension.

In summary, the presented study shows the following:

- In the segment with the preserved articular triad, all layers of the AF decrease in height regardless of the applied load, bulging outward of the IVD.
- Removal of processes from the articular triad of a FSU results in increased mobility within the FSU; those changes are revealed by a greater decrease in height and a greater bulging of the IVD in its anterior or posterior parts in relation to physiological segment.

- Depending on the acting load, the outer layers of the disc become bulged inwards in the anterior (extension) or posterior (flexion) parts.
- Excessive bulging in the anterior or posterior part of the disc in the segment with the posterior column removed is reflected in bigger strain in this area in relation to the physiological segment.

ACKNOWLEDGEMENTS

Calculations have been carried out using resources provided by Wroclaw Centre for Networking and Supercomputing (http://wcss.pl), grant no. 423.

CONFLICT OF INTEREST

We certify that there is no conflict of interest with any financial organisation regarding the material discussed in the manuscript.

DISCLOSURE STATEMENT

No potential conflict of interest was reported by the authors.

ORCID

Klaudia Szkoda-Poliszuk http://orcid.org/0000-0002-3934-2142

REFERENCES

1. White AA, Panjabi MM. *Biomechanical considerations in surgical management of the spine. Clinical Biomechanics of the Spine*. Philadelphia (PA): Lippincot Co.; 1990.
2. Banton RA. Biomechanics of the spine. *J Spinal Res Found* FALL. 2012;7(2):12-20.
3. Rohlmann A, Zander T, Schmidt H, Wilke HJ, Bergmann G. Analysis of the influence of disc degeneration on the mechanical behaviour of a lumbar motion segment using the finite element method. *J Biomech*. 2006;39(13):2484-2490. https://doi.org/10.1016/j.jbiomech.2005.07.026
4. Robertson D, Willardson R, Parajuli D, Cannon A, Bowden AE. The lumbar supraspinous ligament demonstrates increased material stiffness and strength on its ventral aspect. *J Mech Behav Biomed Mater*. 2013;17:34-43. https://doi.org/10.1016/j.jmbbm.2012.07.009
5. Holdsworth F. Fractures, dislocations, and fracture-dislocations of the spine. *J Bone Joint Surg Am*. 1963;45(1):6-20.
6. Nachemson A. Lumbar intradiscal pressure: Experimental studies on post-mortem material. *Acta Orthop Scand Suppl*. 1960;43:1-104.
7. Adams MA, Bogduk N, Burton K, Dolan P. *The biomechanics of back pain*. Toronto (ON): Elsevier Ltd.; 2006.
8. Pollintine P, Przybyla AS, Dolan P, Adams MA. Neural arch loadbearing in old and degenerated spines. *J Biomech*. 2004;37:197-204. https://doi.org/10.1016/S0021-9290(03)00308-7
9. Shirazi-Adl A, Drouin G. Load-bearing role of facets in a lumbar segment under sagittal plane loadings. *J Biomech*. 1987;20(6):601-613.
10. Szkoda K, Pezowicz CA. Finite element analysis of fixation system influence on the thoracolumbar spine stability. *Appl Mech Mater*. 2016;821:685-692. https://doi.org/10.4028/www.scientific.net/AMM.821.685
11. Berry JL, Moran JM, Berg WS, Steffee AD. A morphometric study of human lumbar and selected thoracic vertebrae. *Spine (Phila Pa 1976)*. 1987;12(4):362-367.
12. Panjabi MM, Takata K, Goel V, et al. Thoracic human vertebrae. Quantitative three-dimensional anatomy. *Spine (Phila Pa 1976)*. 1991;16(8):888-901.
13. Panjabi MM, Oxland T, Takata K, Goel V, Duranceau J, Krag M. Articular facets of the human spine. Quantitative three-dimensional anatomy. *Spine (Phila Pa 1976)*. 1993;18(10):1298-1310.
14. Zander T, Rohlmann A, Bergmann G. Influence of different artificial disc kinematics on spine biomechanics. *Clin Biomech*. 2009;24(2):135-142.
15. Lotz JC, Fields AJ, Liebenberg EC. The role of the vertebral endplate in low back pain. *Global Spine J*. 2013;3(3):153-164. https://doi.org/10.1055/s-0033-1347298

16. Shirazi-Adl SA, Shrivastava SC, Ahmed AM. Stress analysis of the lumbar disc-body unit in compression, a three-dimensional nonlinear finite element study. *Spine (Phila Pa 1976)*. 1984;9(2):120-134.

17. Pitzen T, Geisler FH, Matthis D, Müller-Storz H, Pederson K, Steudel WI. The influence of cancellous bone density on load sharing in human lumbar spine: A comparison between an intact and a surgically altered motion segment. *Eur Spine J*. 2001;10(1):23-29. https://doi.org/10.1007/s005860000223

18. Park WM, Kim K, Kim YH. Effects of degenerated intervertebral discs on intersegmental rotations, intradiscal pressures, and facet joint forces of the whole lumbar spine. *Comput Biol Med*. 2013;43(9):1234-1240. https://doi.org/10.1016/j.compbiomed.2013.06.011

19. Zahari SN, Latif MJA, Rahim NRA, Kadir MRA, Kamarul T. The effects of physiological biomechanical loading on intradiscal pressure and annulus stress in lumbar spine: A finite element analysis. *J Healthc Eng*. 2017;2017. 9618940. https://doi.org/10.1155/2017/9618940

20. Zahaf S, Habib H, Mansouri B, Belarbi A, Azari Z. The effect of the eccentric loading on the components of the spine. *Glob J Res Eng*. 2016;4(1):6-22. https://doi.org/10.12691/bse-4-1-2

21. Kurutz M. Finite element modeling of the human lumbar spine. In: *Finite Element Analysis*. InTech; 2010:209-236.

22. Xu M, Yang J, Lieberman IH, Haddas R. Lumbar spine finite element model for healthy subjects: Development and validation. *Comput Methods Biomech Biomed Engin*. 2017;20(1):1-15. https://doi.org/10.1080/10255842.2016.1193596

23. Kim HJ, Tak Kang K, Chang BS, Lee CK, Kim JW, et al. Biomechanical analysis of fusion segment rigidity upon stress at both the fusion and adjacent segments—a comparison between unilateral and bilateral pedicle screw fixation. *Yonsei Med J*. 2014;J55(2):1386-1394. https://doi.org/10.15761/HMO.1000110

24. Lotz JC, Glazer PA, Gryler EC. Tensile properties of the human vertebral endplate. Proceedings of the 22nd Annual Meeting of the International Society for the Study of the Lumbar Spine; Helsinki Finland: International Society for the Lumbar Spine 1995; 21.

25. Kumaresan S, Yoganandan N, Pintar FA. Finite element analysis of the cervical spine: A material property sensitivity study. *Clin Biomech*. 1999;14:41-53. https://doi.org/10.1016/S0268-0033(98)00036-9

26. Keaveny TM, Morgan EF, Niebur GL, Yeh OC. Biomechanics of trabecular bone. *Annu Rev Biomed Eng*. 2001;3(1):307-333. https://doi.org/10.1146/annurev.bioeng.3.1.307

27. Qiu TX, Tan KW, Lee VS, Teo EC. Investigation of thoracolumbar T12–L1 burst fracture mechanism using finite element method. *Med Eng Phys*. 2006;28(7):656-664. https://doi.org/10.1016/j.medengphy.2005.10.011

28. Schmidt H, Galbusera F, Rohlmann A, Zander T, Wilke H. Effect of multilevel lumbar disc arthroplasty on spine kinematics and facet joint loads in flexion and extension: A finite element analysis. *Eur Spine J*. 2012;21(5):663-674. https://doi.org/10.1007/s00586-010-1382-1

29. Ibarz E, Más Y, Mateo J, Lobo-Escolar A, Herrera A, Gracia L. Instability of the lumbar spine due to disc degeneration. A finite element simulation. *Adv Biosci Biotechnol*. 2013;4(04):548-556. https://doi.org/10.4236/abb.2013.44072

30. López E, Elena I, Herrera A, Mateo J, Lobo-Escolar A, et al. Probability of osteoporotic vertebral fractures assessment based on dxa measurements and finite element simulation. *Adv Biosci Biotechnol*. 2014;5(06):527-545. https://doi.org/10.4236/abb.2014.56063

31. Dong R-C, Guo L-X. Human body modeling method to simulate the biodynamic characteristics of spine in vivo with different sitting postures. *Int J Numer Meth Biomed Eng*. 2017;e2876. https://doi.org/10.1002/cnm.2876

32. Li QY, Kim HJ, Son J, et al. Biomechanical analysis of lumbar decompression surgery in relation to degenerative changes in the lumbar spine-validated finite element analysis. *Comput Biol Med*. 2017;89:512-519. https://doi.org/10.1016/j.compbiomed.2017.09.003

33. Shirazi-Adl A, Ahmed AM, Shrivastava SC. A finite element study of a lumbar motion segment subjected to pure sagittal plane moments. *J Biomech*. 1986;19(4):331-350.

34. Polikeit A, Ferguson SJ, Nolte LP, Orr TE. Factors influencing stresses in the lumbar spine after the insertion of intervertebral cages: Finite element analysis. *Eur Spine J*. 2003;12(4):413-420. https://doi.org/10.1007/s00586-002-0505-8

35. Bastian L, Lange U, Knop C, Tusch G, Blauth M. Evaluation of the mobility of adjacent segments after posterior thoracolumbar fixation: A biomechanical study. *Eur Spine J*. 2001;10(4):295-300. https://doi.org/10.1007/s005860100278

36. Wang XY, Dai LY, Xu HZ, Chi YL. Biomechanical effect of the extent of vertebral body fracture on the thoracolumbar spine with pedicle screw fixation: An in vitro study. *J Clin Neurosci*. 2008;15(3):286-290. https://doi.org/10.1016/j.jocn.2006.12.007

37. Panjabi MM, Brand RA, White AA. Mechanical properties of the human thoracic spine as shown by three-dimensional load-displacement curves. *J Bone Joint Surg Am*. 1976;58(5):642-652.

38. Wilke HJ, Wenger K, Claes L. Testing criteria for spinal implants: Recommendations for the standardization of in vitro stability testing of spinal implants. *Eur Spine J*. 1998;7(2):148-154. https://doi.org/10.1007/s005860050045

39. Adams MA, McNally DS, Dolan P. Stress' distributions inside intervertebral discs. The effects of age and degeneration. *J Bone Joint Surg Br*. 1996;76(6):965-972.

40. Żak M. Effect of support on mechanical properties of the intervertebral disc in long-term compression testing. *J Theor Appl Mech*. 2014;52(3):677-686.

41. Pezowicz CA, Robertson PA, Broom ND. The structural basis of interlamellar cohesion in the intervertebral disc wall. *J Anat*. 2006a;208(3):317-330. https://doi.org/10.1111/j.1469-7580.2006.00536.x

42. Pezowicz CA, Schechtman H, Robertson PA, Broom ND. Mechanisms of anular failure resulting from excessive intradiscal pressure: A microstructural-micromechanical investigation. *Spine (Phila Pa 1976)*. 2006b;31(25):2891-2903. https://doi.org/10.1097/01.brs.0000248412.82700.8b

43. Rohlmann A, Neller S, Claes L, Bergmann G, Wilke HJ. Influence of a follower load on intradiscal pressure and intersegmental rotation of the lumbar spine. *Spine (Phila Pa 1976)*. 2001;26(24):557-561. https://doi.org/10.1097/00007632-200112150-00014

44. Wilke HJ, Neef P, Hinz B, Seidel H, Claes L. Intradiscal pressure together with anthropometric data—a data set for the validation of models. *Clin Biomech*. 2001;16:111-126. https://doi.org/10.1016/S0268-0033(00)00103-0

45. Klein JA, Hukins DW. X-ray diffraction demonstrates reorientation of collagen fibres in the annulus fibrosus during compression of the intervertebral disc. *Biochim Biophys Acta*. 1982;717(1):61-64.

46. Heuer F, Schmidt H, Wilke HJ. The relation between intervertebral disc bulging and annular fiber associated strains for simple and complex loading. *J Biomech*. 2008;41(5):1086-1094. https://doi.org/10.1016/j.jbiomech.2007.11.019

47. Denozière G, Ku DN. Biomechanical comparison between fusion of two vertebrae and implantation of an artificial intervertebral disc. *J Biomech*. 2006;39(4):766-775. https://doi.org/10.1016/j.jbiomech.2004.07.039

48. Fredericson M, Lee SU, Welsh J, Butts K, Norbash A, Carragee EJ. Changes in posterior disc bulging and intervertebral foraminal size associated with flexion-extension movement: A comparison between L4–5 and L5–S1 levels in normal subjects. *Spine J*. 2001;1(1):10-17. https://doi.org/10.1016/S1529-9430(01)00014-6

49. Adams MA. Biomechanics of back pain. *Acupunct Med*. 2004;22(1):78-88.

50. Heuer F, Schmitt H, Schmidt H, Claes L, Wilke HJ. Creep associated changes in intervertebral disc bulging obtained with a laser scanning device. *Clin Biomech*. 2007;22(7):737-744. https://doi.org/10.1016/j.clinbiomech.2007.04.010

51. Adams MA, Stefanakis M, Dolan P. Healing of a painful intervertebral disc should not be confused with reversing disc degeneration: Implications for physical therapies for discogenic back pain. *Clin Biomech*. 2010;25(10):961-971. https://doi.org/10.1016/j.clinbiomech.2010.07.016

52. Thalgott JS, Albert TJ, Vaccaro AR, et al. A new classification system for degenerative disc disease of the lumbar spine based on magnetic resonance imaging, provocative discography, plain radiographs and anatomic considerations. *Spine J*. 2004;4(6):167-172. https://doi.org/10.1016/j.spinee.2004.07.001

53. Hilibrand AS, Robbins M. Adjacent segment degeneration and adjacent segment disease: The consequences of spinal fusion? *Spine J*. 2004;4(6 Suppl):190-194. https://doi.org/10.1016/j.spinee.2004.07.007

54. Iorio JA, Jakoi AM, Singla A. Biomechanics of degenerative spinal disorders. *Asian Spine J*. 2006;10(2):377-384. https://doi.org/10.4184/asj.2016.10.2.377

55. Kasis AG, Marshman LA, Krishna M, Bhatia CK. Significantly improved outcomes with a less invasive posterior lumbar interbody fusion incorporating total facetectomy. *Spine (Phila Pa 1976)*. 2009;34(6):572-577. https://doi.org/10.1097/BRS.0b013e3181973e35

56. Lee KK, Teo EC, Qiu TX, Yang K. Effect of facetectomy on lumbar spinal stability under sagittal plane loadings. *Spine (Phila Pa 1976)*. 2004;29(15):1624-1631. https://doi.org/10.1097/01.BRS.0000132650.24437.15

How to cite this article: Szkoda-Poliszuk K, Żak M, Pezowicz C. Finite element analysis of the influence of three-joint spinal complex on the change of the intervertebral disc bulge and height. *Int J Numer Meth Biomed Engng*. 2018;34:e3107. https://doi.org/10.1002/cnm.3107